

A Case-Based Reasoning Method for Discriminating Damage Levels in Ancient Wood Components Based on Fuzzy Similarity Priority

Ziyi Wang,^{a,b} Donghui Ma,^{a,b,c} Wei Wang,^{a,b,*} Wei Qian,^{a,c} Xiaodong Guo,^{a,b,c} Junhong Huan,^d and Zhongwei Gao^{a,b}

In order to rapidly identify internal damage levels accurately in ancient wood components, stress wave detection technology was used to perform simulated damage tests on pine specimens. Based on the detected wave velocity data, the diameter of the specimen, the attenuation coefficient, and the ratio of the wave velocities on the four paths were selected as the discriminant factors for identifying the level of internal damage in the specimens. A case-based reasoning method for discriminating internal damage levels in ancient wood components based on fuzzy similarity priority was proposed. A fuzzy similarity priority relationship between the target case and the source case was established. By introducing the idea of variable weights, the weight of each discriminant factor was determined via the “penalize-excitation” variable weight function. The comprehensive similarity sequences between the target case and the source case were obtained. The source case that was most similar to the target case was used to determine the damage level of the target case. The results showed that this method can quickly and accurately identify the damage levels in ancient wood components, which provides a new method for the safe evaluation of ancient wood buildings.

Keywords: Ancient wood components; Stress wave; Damage level; Case-based reasoning; Fuzzy similarity priority

Contact information: a: Faculty of Architecture, Civil and Transportation Engineering, Beijing University of Technology, Beijing 100124, China; b: Key Scientific Research Base of Safety Assessment and Disaster Mitigation for Traditional Timber Structure (Beijing University of Technology), State Administration for Cultural Heritage, Beijing 100124, China; c: Beijing Engineering Research Center of Historic Buildings Protection, Beijing University of Technology, Beijing 100124, China; d: School of Civil Engineering, Shijiazhuang Tiedao University, Shijiazhuang 050043, China; *Corresponding author: ieeww@bjut.edu.cn

INTRODUCTION

As an important part of ancient Chinese architecture, wood structures are the crystallization of the sweat and wisdom of ancient people and have high historical, artistic, and scientific value. Since most ancient wooden structures are exposed, long-term erosion from natural sources, *e.g.*, wind, rain, and temperature difference, leads to various sources of decay, *e.g.*, moths, damages, and cracks. This not only brings hidden dangers to the structural safety of the whole ancient building, but it also causes the original and true historical information of ancient buildings to gradually disappear (Li 2015). Therefore, it is necessary to obtain accurate information detailing the damage through appropriate and reasonable detection technology, which is of great importance in evaluating the safety and health status of ancient wood structures.

In recent years, great progress has been made in terms of the detection and

protection of ancient wood structures. Among them, as a modern nondestructive testing technology, stress wave testing is widely used in the exploration, analysis, and evaluation of ancient wooden structures. Lee (1965) first used stress wave detection technology to determine the propagation time of lateral stress waves and longitudinal stress waves in wood components, and finally obtained the propagation velocity of the stress waves. Lin and Wu (2013) used the stress wave method to test elm specimens. The results showed that the moisture content of the wood, cracks, size of the holes, and number of holes had significant effects on the expansion parameters and the dynamic elastic modulus. Dackermann *et al.* (2014) used stress waves to measure structural wood properties and proposed how to evaluate the test results and the health status of the analyzed wood components. Li *et al.* (2015) selected six variation factors as the discriminant basis to classify the defect grades of wood components based on the stress wave detection data. Morales-Conde and Machado (2017) predicted the elastic modulus of wood *via* stress wave detection technology considering the spatial variability of wood cross sections. Du *et al.* (2018) proposed a three-dimensional stress wave imaging method based on TKriging to reconstruct internal defect images of wood. Huan *et al.* (2018) proposed a stress wave tomography algorithm with a velocity error correction mechanism based on the wave velocity data set measured *via* stress waves. Finally, a sectional image of the test sample image was generated. Wang *et al.* (2019) used a stress wave and impedance meter to detect the internal damage of wood components, and induced ordered weighted averaging (IOWA) operators, induced ordered weighted geometric averaging (IOWGA) operators, and induced ordered weighted harmonic averaging (IOWHA) operators were introduced to establish a combined prediction model to predict the internal damage of ancient wood structures. Yue *et al.* (2019) compared electric resistance tomography and stress wave tomography for decay detection in trees. The results showed that electric resistance tomography was better than stress wave tomography for testing the early stages of decay, while stress wave tomography was more effective for the late stages of decay. Wang *et al.* (2020) proposed a coupling model of a fuzzy soft set and the Bayesian method to forecast internal defects in wooden structures based on stress waves and an impedance test. Bandara *et al.* (2021) used time-frequency analysis techniques and stress waves to evaluate health monitoring of timber poles.

According to the existing research, when stress waves are used to detect the damage of ancient wood components, the internal damage is generally judged *via* analyzing the 2D image. Although the damage can be qualitatively judged, the analysis process is cumbersome and there is not a high degree of accuracy (Xu *et al.* 2011). There are few scholars who have studied the relationship between the grade of the internal wood damage and the wave velocity of the stress wave. In view of this, the diameter of the specimen, the attenuation coefficient, and the ratio of the wave velocities on the four paths were selected as the discriminant factors for identifying the internal damage levels of specimens. Meanwhile, the concept of fuzzy similarity priority has been introduced to propose case-based reasoning (CBR) for the identification of internal damage in ancient wood components (Zhao and He 2008; He *et al.* 2009; Zhang *et al.* 2015). Concretely speaking, the fuzzy similarity priority relationship between the target case and source case is first established for each discriminant factor. Secondly, the weight of each discriminant factor is determined *via* the “penalize-excitation” variable weight model. Finally, a comprehensive similarity sequence between the target base and source base was obtained to find the source base most similar to the target base. This method can quickly and accurately identify the level of internal damage in ancient wood components.

EXPERIMENTAL

Materials

Pine, which commonly has been used in ancient timber structures, was selected as the test specimen. After visual examination and compression examination, no obvious defects, *e.g.*, joints and cracks, were found in these specimens. The measured average moisture content of the specimens met the requirements of GB/T standard 50005 (2017) and GB/T standard 50329 (2012). Reverse simulation tests were conducted on six specimens, and the simulated type was hollow. The simulated damage ratios were 0, 1/32, 1/16, 1/8, 1/4, and 1/2, respectively. It was assumed that the specimen and the damage shape were a standard complete circle. Table 1 shows the different parameters of the specimens.

Table 1. The Parameters of the Specimens

Specimen Number	Simulated Type	Damage Ratio	Height (cm)	Moisture Content (%)	Detecting Height (cm)	Indoor Temperature (°C)	Air Relative Humidity (%)
Specimen 1 (D = 22 cm)	Hollow	0	10	14.2	5	20	72
Specimen 2 (D = 28 cm)		1/32					
Specimen 3 (D = 34 cm)		1/16					
Specimen 4 (D = 40 cm)		1/8					
Specimen 6 (D = 46 cm)		1/4					
Specimen 6 (D = 520 mm)		1/2					

Stress Wave Detection

A stress wave detector produced by FAKOOP (Ágfalva, Hungary) was used to test these specimens.

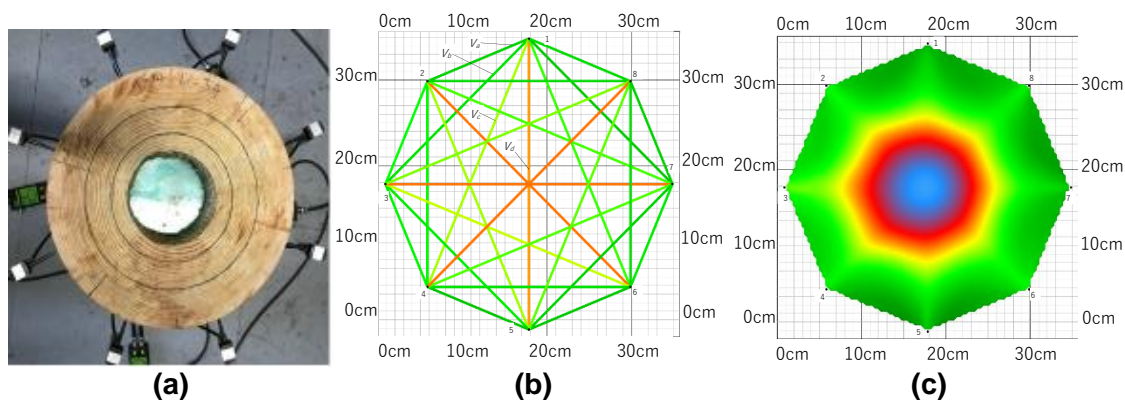


Fig. 1. (a) Stress Wave Detection; (b) Propagation path; and (c) Two-dimensional image

First, eight sensors were selected to place around the specimen using eight steel nails (Fig. 1a). The sensors were connected with a signal amplifier, which could realize wireless connections with a computer *via* Bluetooth. After tapping each sensor with a hammer three times, each sensor transmitted the wave velocity information to the computer through a signal amplifier. Finally, the 2D image of internal damage of the wood was calculated using the ArborSonic 3D software (Version 5.2.107, FAKOPP, Ágfalva, Hungary) (Fig. 1c). Figure 1b shows the propagation path and the 2D image.

Selection of Discriminant Factors and Damage Level

In this experiment, six intact specimens were first tested to obtain the wave velocity value of each path, which was denoted as the initial comparison value V_{m0} ($m = a, b, c, d$). Then, the wave velocities of the specimens were measured using different damage ratios. Wave velocities can be divided into four categories, according to the propagation path (Fig. 1b). Concretely speaking, the wave velocity values between two adjacent points included $V_{a12}, V_{a23}, V_{a34}, V_{a45}, V_{a56}, V_{a67}, V_{a78},$ and V_{a81} , of which the mean values were uniformly denoted as \bar{V}_a . The wave velocity values of two points with one interval included $V_{b13}, V_{b24}, V_{b35}, V_{b46}, V_{b57}, V_{b68}, V_{b71},$ and V_{b82} , of which the mean values were uniformly denoted as \bar{V}_b . The wave velocity values of two points with two intervals included $V_{c14}, V_{c25}, V_{c36}, V_{c47}, V_{c58}, V_{c61}, V_{c72},$ and V_{c83} , of which the mean values were uniformly denoted as \bar{V}_c . The wave velocity values of two points with three intervals included $V_{d15}, V_{d26}, V_{d37},$ and V_{d48} , of which the mean values were uniformly denoted as \bar{V}_d . The attenuation coefficient of the wave velocity (δ_m) can be calculated according to Eq. 1,

$$\delta_m = \frac{|V_{m0}-V|}{V_{m0}} \times 100\% \quad (m = a, b, c, d) \quad (1)$$

(Li 2015).

The ratio of the wave velocity mean values under the four paths were selected as the discriminant factor, which included $\bar{V}_a/\bar{V}_b, \bar{V}_a/\bar{V}_c, \bar{V}_a/\bar{V}_d, \bar{V}_b/\bar{V}_c, \bar{V}_b/\bar{V}_d,$ and \bar{V}_c/\bar{V}_d . Meanwhile, the diameter (D) of the specimen was also taken as a discriminant factor. Therefore, a total of 11 discriminant factors were selected in this model. The classification of the damage level was divided into 6 levels, as shown in Table 2 (Li 2015).

Table 2. Damage Level Classifications

Damage Level	Discriminant Standard
I	No damage
II	$0 < \text{Damage ratio} \leq 1/32$
III	$1/32 < \text{Damage ratio} \leq 1/16$
IV	$1/16 < \text{Damage ratio} \leq 1/8$
V	$1/8 < \text{Damage ratio} \leq 1/4$
VI	$1/4 < \text{Damage ratio} \leq 1/2$

Data Statistics

In this paper, C_1 through C_{36} with known damage levels were taken as training samples to form the source case base. Meanwhile, C_{01} through C_{06} with known damage levels were randomly selected as testing samples to form the target case base. The data statistics of the source and target examples are shown in Table 3.

Table 3. Discriminant Factor Data Statistics

Source Base C_K	Target Base C_0	Discriminant Factor											Damage Level
		X_1	X_2	X_3	X_4	X_5	X_6	X_7	X_8	X_9	X_{10}	X_{11}	
C_1		22	0.000	0.000	0.000	0.000	0.892	0.852	0.856	0.955	0.960	1.005	I
C_2		28	0.000	0.000	0.000	0.000	0.940	0.872	0.866	0.928	0.921	0.993	I
C_3		34	0.000	0.000	0.000	0.000	0.949	0.932	0.950	0.982	1.001	1.019	I
C_4		40	0.000	0.000	0.000	0.000	0.944	0.948	0.975	1.004	1.033	1.029	I
C_5		46	0.000	0.000	0.000	0.000	1.051	1.085	1.135	1.032	1.079	1.046	I
C_6		52	0.000	0.000	0.000	0.000	0.977	1.015	1.040	1.039	1.065	1.025	I
C_7		22	0.041	0.017	0.035	0.083	0.914	0.919	0.972	1.006	1.064	1.058	II
C_8		28	0.015	0.002	0.079	0.140	0.957	0.962	1.022	1.005	1.068	1.062	II
C_9		34	0.055	0.021	0.019	0.034	0.981	1.003	1.037	1.023	1.058	1.034	II
C_{10}		40	0.023	0.035	0.078	0.102	0.956	1.005	1.061	1.051	1.110	1.056	II
C_{11}		46	0.034	0.023	0.011	0.027	1.063	1.109	1.206	1.043	1.134	1.087	II
C_{12}		52	0.051	0.068	0.092	0.149	0.995	1.060	1.159	1.066	1.166	1.094	II
C_{13}		22	0.031	0.004	0.091	0.165	0.924	0.966	1.058	1.045	1.144	1.095	III
C_{14}		28	0.009	0.023	0.147	0.237	0.971	1.032	1.144	1.063	1.178	1.109	III
C_{15}		34	0.036	0.137	0.018	0.051	0.805	0.916	0.965	1.138	1.199	1.054	III
C_{16}		40	0.033	0.011	0.074	0.129	0.986	1.057	1.156	1.072	1.173	1.094	III
C_{17}		46	0.067	0.054	0.031	0.009	1.065	1.122	1.200	1.054	1.127	1.069	III
C_{18}		52	0.019	0.024	0.073	0.136	1.020	1.115	1.227	1.093	1.203	1.101	III
C_{19}		22	0.046	0.032	0.170	0.280	0.964	1.074	1.244	1.114	1.290	1.159	IV
C_{20}		28	0.029	0.031	0.196	0.308	0.998	1.115	1.285	1.117	1.288	1.153	IV
C_{21}		34	0.035	0.026	0.144	0.242	1.008	1.126	1.296	1.118	1.286	1.151	IV
C_{22}		40	0.051	0.016	0.123	0.205	1.009	1.136	1.289	1.126	1.278	1.135	IV
C_{23}		46	0.056	0.045	0.006	0.023	1.062	1.139	1.227	1.072	1.155	1.077	IV
C_{24}		52	0.009	0.079	0.152	0.205	1.052	1.186	1.296	1.127	1.232	1.093	IV
C_{25}		22	0.048	0.079	0.255	0.378	1.016	1.199	1.443	1.180	1.420	1.203	V
C_{26}		28	0.037	0.052	0.253	0.382	1.028	1.210	1.452	1.177	1.412	1.200	V
C_{27}		34	0.093	0.006	0.162	0.210	1.043	1.215	1.313	1.165	1.259	1.080	V
C_{28}		40	0.080	0.026	0.163	0.188	1.047	1.223	1.296	1.169	1.238	1.060	V
C_{29}		46	0.029	0.027	0.056	0.135	1.053	1.182	1.349	1.123	1.281	1.141	V
C_{30}		52	0.002	0.108	0.237	0.255	1.093	1.327	1.393	1.214	1.275	1.050	V
C_{31}		22	0.101	0.269	0.424	0.519	1.096	1.328	1.600	1.212	1.460	1.205	VI
C_{32}		28	0.075	0.259	0.428	0.529	1.172	1.410	1.697	1.203	1.448	1.204	VI
C_{33}		34	0.001	0.134	0.306	0.391	1.095	1.342	1.557	1.226	1.422	1.160	VI
C_{34}		40	0.191	0.288	0.392	0.436	1.073	1.261	1.397	1.175	1.302	1.108	VI
C_{35}		46	0.019	0.003	0.151	0.286	1.068	1.301	1.618	1.219	1.516	1.244	VI
C_{36}		52	0.281	0.412	0.552	0.564	1.194	1.628	1.713	1.363	1.435	1.053	VI
	C_{01}	22	0.035	0.017	0.037	0.089	0.908	0.913	0.969	1.006	1.067	1.061	II
	C_{02}	22	0.058	0.015	0.153	0.266	0.958	1.061	1.229	1.107	1.283	1.159	IV
	C_{03}	28	0.035	0.010	0.131	0.223	0.973	1.031	1.149	1.060	1.181	1.114	III
	C_{04}	28	0.067	0.035	0.238	0.369	1.029	1.213	1.460	1.179	1.418	1.203	V
	C_{05}	34	0.000	0.000	0.000	0.000	0.952	0.935	0.952	0.982	1.000	1.018	I
	C_{06}	34	0.088	0.089	0.280	0.398	1.138	1.412	1.720	1.241	1.511	1.218	VI

Note: X_1 represents the diameter D (cm); X_2 through X_5 represents δ_a , δ_b , δ_c , and δ_d , respectively; X_6 through X_{11} represents \bar{V}_a/\bar{V}_b , \bar{V}_a/\bar{V}_c , \bar{V}_a/\bar{V}_d , \bar{V}_b/\bar{V}_c , \bar{V}_b/\bar{V}_d , and \bar{V}_d/\bar{V}_d respectively.

Model Construction

It can be seen in Table 3 that there are many discriminant factors and there is a high degree of nonlinearity between these discriminant factors. It is debatable whether simply relying on a certain discriminant factor to determine the damage level of the target case is suitable. In response to this, this section tentatively proposes a case-based reasoning method for determining the internal damage level of ancient wood components based on a fuzzy similarity priority ratio.

Fuzzy analogy preferred ratio

Suppose A is a set with K objects in the domain U , where $A = \{a_1, a_2, \dots, a_K\}$, $\forall a_i, a_j \in A$ ($i, j = 1, 2, \dots, K$). Let a_i and a_j compare with object a_0 , then the fuzzy similarity priority relationship R is the following mapping shown in Eq. 2,

$$\begin{cases} R = (r_{ij})_{K \times K}, r_{ij} \in [0, 1], (i, j = 1, 2, \dots, K) \\ R: A \times A \rightarrow [0, 1] \end{cases} \quad (2)$$

where, $\gamma_{ij} + \gamma_{ji} = 0$ ($i \neq j, i, j = 1, 2, \dots, K$), $\gamma_{ii} = 0$ ($i = 1, 2, \dots, K$) (Liu and Zhu 2002).

The above conditions indicate that if a_i is compared with itself, there is no so-called priority, and $\gamma_{ii} = 0$. If a_i has a priority of γ_{ij} when compared with a_j , then a_j has a priority of $\gamma_{ji} = 1 - \gamma_{ij}$ when compared with a_i . If $\gamma_{ij} = 1$, it means that a_i is much more similar to a_0 than a_j . If $\gamma_{ij} = 0.5$, it means that a_i and a_j are the same degree of similarity to a_0 . Therefore, γ_{ij} is called the fuzzy similarity priority ratio of a_i similar to a_0 when compared with a_j , and R is called the fuzzy similarity priority relationship.

Representation of the source case and target case

Suppose $B = B_1 \times B_2 \times \dots \times B_j \times \dots \times B_n$ is a n -dimensional factor discrete space and B_j ($j = 1, 2, \dots, n$) is a finite real number set. The case can be defined as $C = (b_1, b_2, \dots, b_j, \dots, b_n)$, where, $b_j \in B_j$ ($j = 1, 2, \dots, n$) and b_j is the discriminant factor of the source case. Correspondingly, the source case can be expressed as $BC = \{C_1, C_2, \dots, C_k, \dots, C_K\}$, where $C_k \in BC$ ($k = 1, 2, \dots, K$) and C_k is the source case. Then, the target case can be expressed as $C_0 = (b_{01}, b_{02}, \dots, b_{0j}, \dots, b_{0n})$, where b_{0j} ($j = 1, 2, \dots, n$) is the discriminant factor of the target case.

Similarity measure between discriminant factors

Suppose C_p and C_q are the source cases, where, $C_p, C_q \in BC$, $C_p \neq C_q$. C_0 is the target case, leading to Eq. 3, Eq. 4, and Eq. 5,

$$C_p = (b_{p1}, b_{p2}, \dots, b_{pj}, \dots, b_{pn}) \quad (3)$$

$$C_q = (b_{q1}, b_{q2}, \dots, b_{qj}, \dots, b_{qn}) \quad (4)$$

$$C_0 = (b_{01}, b_{02}, \dots, b_{0j}, \dots, b_{0n}) \quad (5)$$

The similarity measurement between the discriminant factors can be expressed by the semantic distance between the discriminant factors, which can be solved using the Hamming distance formula. The semantic distance between the j -th discriminant factor of C_p and the j -th discriminant factor of C_0 is expressed as Eq. 6,

$$D(C_{pj}, C_{0j}) = |b_{pj} - b_{0j}| \quad (6)$$

and the semantic distance between the j -th discriminant factor of C_q and the j -th discriminant factor of C_0 is expressed as Eq. 7,

$$D(C_{qj}, C_{0j}) = |b_{qj} - b_{0j}| \quad (7)$$

where, $D(C_{pj}, C_{0j})$ is the semantic distance between the j -th discriminant factor b_{pj} of C_p and the j -th discriminant factor b_{0j} of C_0 . $D(C_{qj}, C_{0j})$ is the semantic distance between the j -th discriminant factor b_{qj} of C_q and the j -th discriminant factor b_{0j} of C_0 .

When the semantic distance between the two cases is used to indicate the similarity degree, it can be considered that the smaller the semantic distance is, the more similar the two discriminant factors are.

Constructing the fuzzy similarity priority relationship

The fuzzy similarity priority ratio of C_{pj} similar to C_{0j} when compared with C_{qj} can be defined as Eq. 8,

$$D_{pq}^j = \frac{D(C_{qj}, C_{0j})}{D(C_{pj}, C_{0j}) + D(C_{qj}, C_{0j})} \quad (8)$$

where $D_{pq}^j \in [0, 1]$, $D_{qp}^j = 1 - D_{pq}^j \in [0, 1]$. The bigger D_{pq}^j is, the bigger the similarity degree of C_{pj} similar to C_{0j} when compared with C_{qj} is.

The fuzzy similarity priority relationship $D(j)$ corresponding to the j -th discriminant factor can be constructed by the following steps:

Taking p and q equal to $1, 2, \dots, K$ in turn, if $p = 1$, and $q = 2, 3, \dots, K$, $D_{12}^j, D_{13}^j, \dots, D_{1K}^j$ is solved. If $p = 2$ and $q = 1, 3, \dots, K$, $D_{22}^j, D_{23}^j, \dots, D_{2K}^j$ is solved. Meanwhile, if p is equal to q , then $D_{pq}^j = 1$. Finally, the matrix $D(j)$ can be expressed as Eq. 9,

$$D(j) = \begin{bmatrix} 1 & D_{12}^j & \dots & D_{1K}^j \\ D_{21}^j & 1 & \dots & D_{2K}^j \\ \dots & \dots & \dots & \dots \\ D_{K1}^j & D_{K2}^j & \dots & 1 \end{bmatrix} \quad (j = 1, 2, \dots, n) \quad (9)$$

where the matrix is called the fuzzy similarity priority relationship of the j -th discriminant factor. By taking j equal to $1, 2, \dots, n$, in turn, the n fuzzy similarity precedence relationships corresponding to the n discriminant factors can be obtained.

Discriminating the level of internal damage in ancient wood components based on fuzzy similarity priority

Taking a λ -cut set for $D(j)$, the K similarity degree sequences between the j -th discriminant factor of the source cases and the target case C_0 is obtained. Let λ be from big to small to check C_0 , respectively. If the elements on the p -th row are all 1 (except for the elements on the diagonal, which are 0), it can be considered that C_p and C_0 are most similar. At this point, the row and column where C_p is located are deleted. By that analogy, the similarity degree sequences between the K source cases and C_0 can be obtained.

Suppose that the source case that is most similar to the target case C_0 is listed at the top of the sequence and its sequence number is 1 and the source sample that is least similar to the target case C_0 is listed at the end of the sequence and its sequence number K . Then, the sequence numbers of the K source cases can constitute the following sequence number set, shown in Eq. 10,

$$T_j = (t_{1j}, t_{2j}, \dots, t_{kj}, \dots, t_{Kj}) \quad (10)$$

There are n sequence number sets corresponding to n discriminant factors, as shown in Eq. 11,

$$\left. \begin{aligned} T_1 &= (t_{11}, t_{21}, \dots, t_{K1}) \\ T_2 &= (t_{12}, t_{22}, \dots, t_{K2}) \\ &\dots \\ T_n &= (t_{1n}, t_{2n}, \dots, t_{Kn}) \end{aligned} \right\} \quad (11)$$

The sequence number of the similarity degree between the k -th source case and the target case C_0 can be expressed as Eq. 12,

$$F_k = \sum_{j=1}^n \omega_j \times t_{kj} \quad (12)$$

where ω_j is the weight of n discriminant factors. Taking k equal to $1, 2, \dots, K$, in turn, the sequence number of K source cases can be obtained by using Eq. 12. The smaller F_k is, the more similar C_k and C_0 is.

Establishment of the variable weight model

Weights are used to measure the relative importance of influencing factors. Considering the sensitivity of the weights, the same factor will have different influences on the decision output in different decision-making environments (Zhou *et al.* 2010). During the determination of the weight (ω_j) of the discriminant factor, whether the weight selection is reasonable or not directly determines the accuracy of the discriminant result. However, the evaluation method adopted by the current evaluation standard is a constant weight evaluation method, *i.e.*, regardless of how the value of the discriminant factors change, the weights of the discriminant factors are constant. If one or two discriminant factors are particularly dangerous, it may be neutralized by other discriminant factor regardless of the utilized evaluation method. This may reduce the accuracy of the evaluation system and decrease the objective impartiality of the evaluation.

In addition, the more discriminant factors there are, the more average the weights are. Therefore, the greater the possibility of misjudgment (Liu 2010). To verify whether the evaluation results were consistent, this paper introduced entropy weight (Zhou *et al.* 2010), fractal theory (Liu *et al.* 2005), and projection pursuit (Wang 2019) to determine the weights (ω_j) of the discriminant factors, respectively. In the terms of the limitations of the constant weight method, three variable weight evaluation models integrating “penalize” and “excitation” were established to improve these three constant weight methods, respectively. The variable weight model can effectively solve the unreasonable evaluation results caused by multiple discriminant factors. According to the principle of state variable weight, the state variable weight vector (S) can be expressed as Eq. 13,

$$S = (s_1, s_2, \dots, s_j, \dots, s_n) \quad (j = 1, 2, \dots, n) \quad (13)$$

where s_j is the function of x_j , which can be determined by Eq. 14,

$$s_j = \begin{cases} \frac{c_1 - c_2}{\lambda - \mu} \mu \ln \frac{\mu}{x_j} + c^2, & 0 < x_j \leq \mu \\ -\frac{c_1 - c_2}{\lambda - \mu} x_j + \frac{c_2 \lambda - c_1 \mu}{\lambda - \mu}, & \mu < x_j \leq \lambda \\ C + \frac{c_1 - c_2}{2(\lambda - \mu)(\alpha - \lambda)} (\alpha - x_j)^2, & \lambda < x_j \leq \alpha \\ C, & \alpha < x_j \leq \beta \\ R(1 - \beta) \ln \frac{1 - \beta}{1 - x_j} + C, & \beta < x_j < 1 \end{cases} \quad (14)$$

where s_j is a state variable weight function of the penalize-excitation, x_j is the state value of each discriminant factor of the target case, which can be obtained by normalizing 11 discriminant factors, α is the level of “penalize”, β is the level of “excitation”, C , c_1 , and c_2 are the evaluation strategies, and R is the adjustment factor (Duan 2003; Fan and Chen (2008). These parameters need to meet two conditions: $0 < \mu < \lambda < \alpha < \beta < 1$ and $0 < C < c_1 < c_2 < 1$.

The characteristics of the variable weight evaluation are specifically reflected in the following three aspects:

(1) For the evaluation value of each discriminant factor, there is $x_j \in (0,1)$. The closer the level of “excitation” β is to 1, *i.e.*, the narrower the interval $(\beta, 1)$, the faster the strong “excitation” that the state in this interval receives is.

(2) If the level of “penalize” α is very close to the level of “excitation” β , *i.e.*, the qualified interval $[\alpha, \beta]$ is narrow, then there is neither “penalize” nor “excitation” for the state in this interval.

(3) The interval $(0, \alpha)$ of “penalize” is wide and is divided into three stages, including the initial “penalize” stage (λ, α) , the strong “penalize” stage $(\mu, \lambda]$, and the veto stage $(0, \mu]$. The level of “penalize” that the state receives is low during the initial “penalize” stage, while the level of “penalize” that the state receives is large during the strong “penalize” stage. In the veto stage, the evaluation value of the evaluation project is too low, but it has a large weight; therefore, the overall evaluation value of the overall target sharply drops. When the evaluation value is lower than or equal to the specified veto value, the entire target will be rejected.

If $0 < C < 1$, $0 < 1-\beta < C$, $\frac{c_1-c_2}{\lambda-\mu} > \frac{1-C}{\alpha}$, and $1 < R < \frac{C}{1-\beta}$, then s_j is a state variable weight function of the strong local penalize-excitation (Duan 2003). According to s_j , the variable weight model can be obtained according to Eq. 15,

$$\omega_j = \frac{\omega'_j s_j}{\sum_{k=1}^n \omega'_k s_k} \quad (15)$$

Combining Eq. 15 into Eq. 12 to obtain the weighted sum F_k ($k = 1, 2, \dots, K$) of the sequence number of all source cases in K sequences yields Eq. 16,

$$F_k = \sum_{j=1}^n \frac{\omega'_j s_j}{\sum_{k=1}^n \omega'_k s_k} \times t_{kj} \quad (16)$$

RESULTS AND DISCUSSION

Determining the Similarity Degree Sequence

Taking the target case C_{01} as an example to illustrate the discriminating process, the fuzzy similarity relations $D(1)$ corresponding to 11 discriminant factors can be established according to Eqs. 6 through 9. Simultaneously, the similarity priority matrix of each discriminant factor was established, which was represented by $D(j)$ ($j = 1, 2, \dots, 11$). Secondly, the similarity degree sequence T_j ($j = 1, 2, \dots, 11$) between each discriminant factor of the source cases and each discriminant factor of the target case C_{01} could be obtained by using the obtained fuzzy similarity priority relationship $D(j)$, which is shown in Table 4.

Table 4. The Similarity Degree Sequence between the Target Case C_{01} and Source Cases C_1 Through C_{36}

Source Case	Similarity Degree Sequence (t_{kj})										
	X_1	X_2	X_3	X_4	X_5	X_6	X_7	X_8	X_9	X_{10}	X_{11}
C_1	1	28	15	27	30	19	30	33	34	35	35
C_2	2	28	15	27	30	8	28	31	35	36	36
C_3	3	28	15	27	30	4	21	29	33	34	34
C_4	4	28	15	27	30	6	18	26	28	33	32
C_5	5	28	15	27	30	23	4	15	23	27	30
C_6	6	28	15	27	30	7	6	21	20	29	33
C_7	1	8	2	20	22	14	23	27	26	30	25
C_8	2	22	14	12	16	1	17	23	27	28	23
C_9	3	2	4	22	24	9	11	22	24	31	31
C_{10}	4	19	18	13	20	2	10	19	14	25	26
C_{11}	5	14	5	24	25	27	7	4	18	21	18
C_{12}	6	3	22	10	14	12	1	11	11	15	15
C_{13}	1	16	10	11	11	11	16	20	17	19	14
C_{14}	2	24	6	3	5	5	5	14	12	13	11
C_{15}	3	12	27	23	23	34	24	28	8	12	27
C_{16}	4	15	3	14	19	10	2	12	10	14	16
C_{17}	5	5	21	21	28	28	12	5	13	23	22
C_{18}	6	20	7	15	17	18	8	1	4	11	13
C_{19}	1	7	17	7	2	3	3	3	1	5	1
C_{20}	2	17	16	9	6	13	9	6	2	4	3
C_{21}	3	13	9	5	4	15	13	10	3	2	4
C_{22}	4	4	1	8	8	16	14	7	6	3	6
C_{23}	5	1	19	25	26	26	15	2	9	16	20
C_{24}	6	25	24	1	9	24	20	9	7	10	17
C_{25}	1	6	23	19	12	17	22	24	22	18	8
C_{26}	2	10	20	18	13	20	25	25	21	17	7
C_{27}	3	18	8	4	7	21	26	13	15	8	19
C_{28}	4	11	11	6	10	22	27	8	16	9	24
C_{29}	5	17	13	17	18	25	19	16	5	1	5
C_{30}	6	26	25	16	1	31	32	17	30	6	29
C_{31}	1	23	29	29	27	33	33	32	29	26	10
C_{32}	2	9	28	30	29	35	35	35	25	24	9
C_{33}	3	27	26	26	15	32	34	30	32	20	2
C_{34}	4	29	30	28	21	30	29	18	19	7	12
C_{35}	5	21	12	2	3	29	31	34	31	32	21
C_{36}	6	30	31	31	31	36	36	36	36	22	28

Determining the Weights of the Discriminant Factors

The fractal theory was taken as an example to illustrate the construction process of the variable weight model of the discriminant factors. The discriminant factors of the target case C_{01} were normalized to obtain the state value of each discriminant factor of the target case C_{01} . According to the characteristics of the source cases, let $\mu = 0.2$, $\lambda = 0.6$, $\alpha = 0.7$, $\beta = 0.9$, $C = 0.5$, $c_1 = 0.5$, $c_2 = 0.8$, and $R = 1.3$; under these conditions, the state variable weight function of the local penalize-excitation is expressed as Eq. 17

$$s_j = \begin{cases} 0.15\ln\frac{0.2}{x_j} + 0.8, 0 < x_j \leq 0.2 \\ -0.75x_j + 0.95, 0.2 < x_j \leq 0.6 \\ 2.3375 - 5.25x_j + x_j^2, 0.6 < x_j \leq 0.7 \\ 0.5, 0.7 < x_j \leq 0.9 \\ 0.13\ln\frac{0.1}{1-x_j} + 0.5, 0.9 < x_j < 1 \end{cases} \quad (17)$$

According to Eq. 15, the weights (ω_j) of the discriminant factors based on the fractal theory can be obtained *via* the variable weight model. Similarly, the weights (ω_j) of each discriminant factor based on entropy weights and projection pursuits can be calculated, as shown in Table 5.

Table 5. The Weights of the Discriminant Factors of the Target Case C_{01}

Methods	ω_j										
	X_1	X_2	X_3	X_4	X_5	X_6	X_7	X_8	X_9	X_{10}	X_{11}
Entropy weight	0.320	0.058	0.097	0.098	0.101	0.032	0.058	0.073	0.046	0.057	0.059
Fractal theory	0.095	0.098	0.105	0.101	0.090	0.080	0.095	0.093	0.088	0.076	0.079
Projection pursuit	0.117	0.075	0.108	0.115	0.101	0.071	0.099	0.098	0.082	0.079	0.054

Determining the Comprehensive Similarity Sequence

The comprehensive similarity sequence (F_k) of the target case C_{01} was obtained using Eq. 16, which is shown in Table 6. As shown in Fig. 2, it can be found that the F_k corresponding to the source case C_7 obtained by the three weight determination methods is the minimum. Since the smaller F_k is, the more similar the source case and target case C_{01} is. The results show that the target case C_{01} is most similar to the source case C_7 , as shown in Table 6. In addition, C_7 represents a source case with a diameter of 22 cm and has a damage level of II. It can be concluded that the damage level of target case C_{01} is also II.

Similarly, the comprehensive similarity sequence (F_k) between the other target cases and the source cases can be quickly obtained through the above discriminant steps. In order to intuitively represent the discriminant results, Figs. 2 through 7 show the comprehensive similarity sequence (F_k) histograms between target cases C_{01} through C_{06} and source cases C_1 through C_{36} .

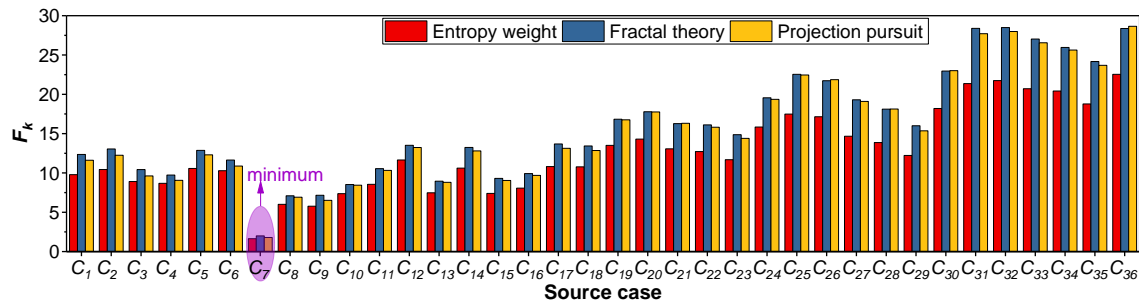


Fig. 2. The F_k histogram between target case C_{01} and source cases C_1 through C_{36}

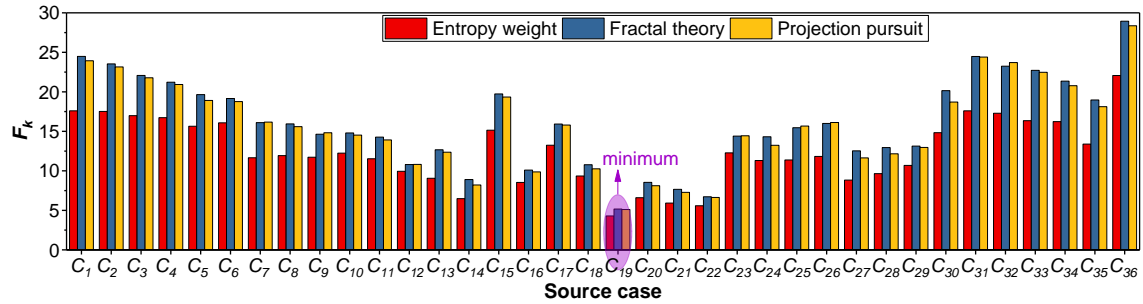


Fig. 3. The F_k histogram between target case C_{02} and source cases C_1 through C_{36}

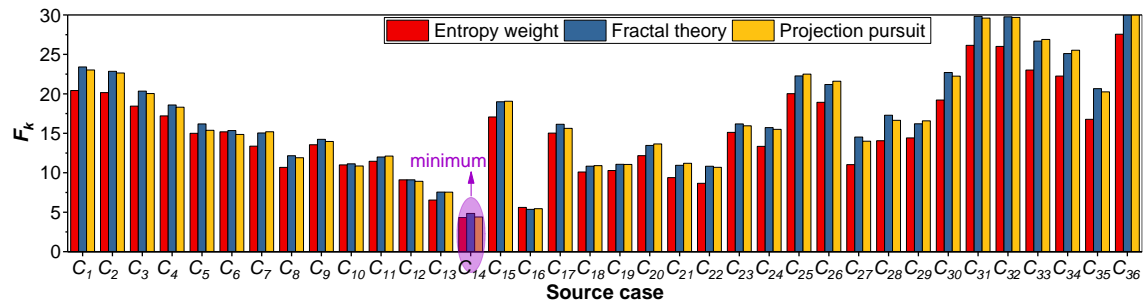


Fig. 4. The F_k histogram between target case C_{03} and source cases C_1 through C_{36}

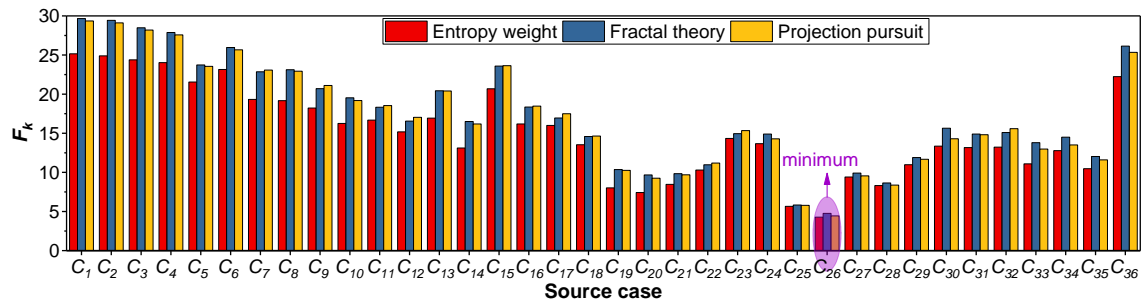


Fig. 5. The F_k histogram between target case C_{04} and source cases C_1 through C_{36}

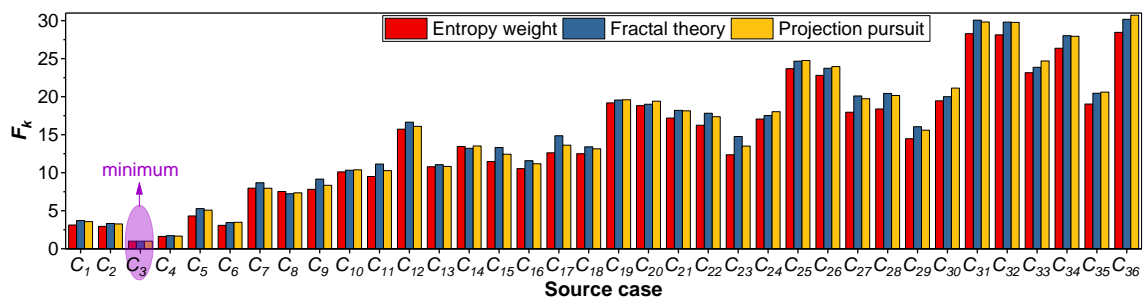


Fig. 6. The F_k histogram between target case C_{05} and source cases C_1 through C_{36}

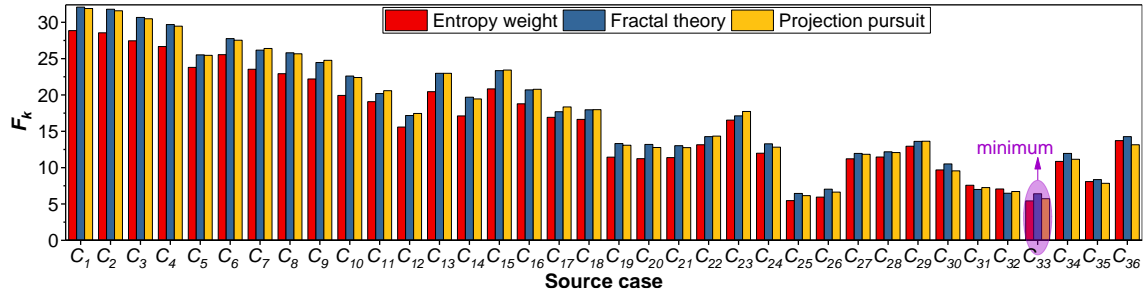


Fig. 7. The F_k histogram between target case C_{06} and source cases C_1 through C_{36}

Table 6. The Comprehensive Similarity Sequence (F_k) of Target Case C_{01} and the Source Cases C_1 through C_{36}

Source Case	F_k		
	Entropy Weight	Fractal Theory	Projection Pursuit
C_1	9.781	12.352	11.617
C_2	10.435	13.049	12.250
C_3	8.906	10.431	9.622
C_4	8.680	9.730	9.057
C_5	10.572	12.873	12.300
C_6	10.285	11.642	10.880
C_7	1.639	1.995	1.791
C_8	6.007	7.095	6.914
C_9	5.766	7.163	6.519
C_{10}	7.368	8.523	8.443
C_{11}	8.553	10.544	10.324
C_{12}	11.647	13.514	13.237
C_{13}	7.474	8.948	8.810
C_{14}	10.613	13.241	12.805
C_{15}	7.397	9.304	9.042
C_{16}	8.065	9.922	9.689
C_{17}	10.810	13.683	13.136
C_{18}	10.776	13.431	12.853
C_{19}	13.509	16.833	16.759
C_{20}	14.305	17.786	17.759
C_{21}	13.068	16.271	16.314
C_{22}	12.714	16.108	15.811
C_{23}	11.681	14.868	14.399
C_{24}	15.837	19.559	19.358
C_{25}	17.489	22.545	22.457
C_{26}	17.147	21.730	21.867
C_{27}	14.669	19.301	19.100
C_{28}	13.859	18.115	18.129
C_{29}	12.225	15.999	15.359
C_{30}	18.201	22.956	23.005
C_{31}	21.364	28.389	27.711
C_{32}	21.743	28.488	27.992
C_{33}	20.706	27.032	26.554
C_{34}	20.421	25.960	25.633
C_{35}	18.778	24.172	23.692
C_{36}	22.542	28.367	28.653

It can be obviously seen from Figs. 2 through 7 that the source cases corresponding to the minimum value of the F_k obtained by the three weighting methods were C_7 , C_{19} , C_{14} , C_{26} , C_3 , and C_{33} , respectively. The smaller the weighted sum F_k is, the more similar the source case and target case is. Table 7 shows the discriminant result of damage levels of the target cases C_{01} through C_{06} . The discriminant results of the model used in this paper are all in line with the actual situation, and the discrimination accuracy is 100%. The case analysis shows that the method has simple reasoning principle and reliable results, which provides a quick and accurate method to discriminate the internal damage of ancient wooden components.

Table 7. Discriminant Result of Damage Levels of the Target Cases C_{01} through C_{06}

Target Base	Methods	$\min F_k$	Source Base Corresponding to $\min F_k$	Damage Level of Source Base	Actual Damage Level	Discriminant Result
C_{01}	Entropy Weight	1.639	C_7	II	II	II
	Fractal Theory	1.995	C_7	II		
	Projection Pursuit	1.791	C_7	II		
C_{02}	Entropy Weight	4.297	C_{19}	IV	IV	IV
	Fractal Theory	5.166	C_{19}	IV		
	Projection Pursuit	5.109	C_{19}	IV		
C_{03}	Entropy Weight	4.329	C_{14}	III	III	III
	Fractal Theory	4.842	C_{14}	III		
	Projection Pursuit	4.394	C_{14}	III		
C_{04}	Entropy Weight	4.272	C_{26}	V	V	V
	Fractal Theory	4.760	C_{26}	V		
	Projection Pursuit	4.440	C_{26}	V		
C_{05}	Entropy Weight	1.000	C_3	I	I	I
	Fractal Theory	1.000	C_3	I		
	Projection Pursuit	1.000	C_3	I		
C_{06}	Entropy Weight	5.428	C_{33}	VI	VI	VI
	Fractal Theory	6.408	C_{33}	VI		
	Projection Pursuit	5.726	C_{33}	VI		

Limitations

This study has certain limitations. This test only simulates the damage type of the hollow through a single symmetrical circle for a wood component of one tree species. A variety of damage conditions (such as decay, cracks, insect attacks, *etc.*) need to be considered in the follow-up study. Meanwhile, a sample database of different tree species can be established to enhance the applicability of the model. In addition, the discrimination of internal damage of ancient wooden components is not only related to the wave speed, but also affected by other factors. The selection of discriminant factors needs to be studied in depth.

CONCLUSIONS

1. In the study, three discriminant factors, *i.e.*, diameter, attenuation coefficient, and wave velocity ratio, were selected based on the stress wave detection data. In addition, the concept of fuzzy similarity priority was introduced to establish a case-based reasoning method for determining the internal damage levels of ancient wood components based on fuzzy similarity priority. Through the comparison of different discriminant factors between the target case and the source case, a reasonable reasoning relationship between them was established. This relationship was established to find the most similar source case to the target case, in order to realize the discrimination of the level of internal damage to the ancient wooden components. This method had a simple reasoning principle, high efficiency, as well as stable and reliable calculation results. Therefore, it can provide a feasible new way for the health assessment of ancient building wood components.
2. When determining the weight of a discriminant factor, this paper introduces the idea of variable weight; as such, the state variable weight functions of the local penalize-excitation based on three weighting methods which include entropy weight, fractal theory, and projection pursuit were established, respectively. The results show that the weight distribution of the discriminant factors obtained via the variable models had good consistency, improved the accuracy of the discrimination system, and ensured the objectivity and fairness of the judgment results.

ACKNOWLEDGMENTS

This study was supported by the National Key R&D Program of China (Grant No. 2018YFD1100902-1), the Beijing Municipal Commission of Education-Municipal Natural Science Joint Foundation (Grant No. KZ202010005012) and the National key research and development program (Grant No. 2019YFC1520803).

REFERENCES CITED

- Bandara, S., Rajeev, P., Gad, E., Sriskantharajah, B., and Flatley, I. (2021). "Health monitoring of timber poles using time-frequency analysis techniques and stress wave propagation," *Journal of Civil Structural Health Monitoring* 11(1). 85-103. DOI: 10.1007/s13349-020-00440-1
- Dackermann, U., Crews, K., Kasal, B., Li, J., Riggio, M., Rinn, F., and Tannert, T. (2014). "In situ assessment of structural timber using stress-wave measurements," *Materials and Structures* 47(5), 787-803. DOI: 10.1617/s11527-013-0095-4
- Duan, S.-Q. (2003). "A method of variable weight synthetic evaluation for safety management of power business," *Mathematics in Practice and Theory* 8, 17-23.
- Du, X., Feng, H., Hu, M., Fang, Y., and Chen, S. (2018). "Three-dimensional stress wave imaging of wood internal defects using TKriging method," *Computers and Electronics in Agriculture* 148, 63-71. DOI: 10.1016/j.compag.2018.03.005
- Fan, M.-F. and Chen, G.-H. (2008). "Study on risk assessment method of gas-fired power plant based on variable weight model," *Gas & Heat* 24(4), 78-83.

- GB/T 50329 (2012). "Standard for test methods of timber structures," Standardization Administration of China, Beijing, China.
- GB 50005 (2017). "Standard for design of timber structures," Standardization Administration of China, Beijing, China.
- He, H., Wen, K., Chen, Z., and Ye, W. (2009). "Case-based reasoning and fuzzy analogy preferred ratio for effective depth of collapsible loess treated with dynamic consolidation," *Journal of Engineering Geology* 17(1), 88-93.
- Huan, Z., Jiao, Z., Li, G., and Wu, X. (2018). "Velocity error correction based tomographic imaging for stress wave nondestructive evaluation of wood," *BioResources* 13(2), 2530-2545. DOI: 10.15376/biores.13.2.2530-2545
- Lee, L. D. (1965). "Ultrasonic pulse velocity testing considered as a safety measure for timber structures," in: *Proceedings of the 2nd Nondestructive Testing of Wood Symposium*, Spokane, WA, USA, pp. 185-203.
- Liu, M., and Zhu, R. (2002). "Case-based reasoning approach to slope stability evaluation based on fuzzy analogy preferred ratio," *Chinese Journal of Rock Mechanics and Engineering* 21(8), 1188-1193.
- Liu, G.-P., Du, P., and Wang, K. (2005). "Application of fractal theory to evaluation of lake eutrophication," *Acta Agriculturae Universitatis Jiangxiensis* 27(6), 925-929.
- Liu, K. (2010). "A synthesis evaluation method for highway pavement based on a variable weight model," *Journal of Xiamen University (Natural Science)* 49(4), 531-534.
- Lin, W. S., and Wu, J. Z. (2013). "Study on application of stress wave for nondestructive test of wood defects," *Applied Mechanics and Materials* 401-403, 1119-1123. DOI: 10.4028/www.scientific.net/AMM.401-403.1119
- Li, X., Dai, J., Qian, W., and Chang, L.-H. (2015). "Prediction of internal defect area in wooden components by stress wave velocity analysis," *BioResources* 10(3), 4167-4177. DOI: 10.15376/biores.10.3.4167-4177
- Li, X. (2015). *Key Technology Research on Material Performance and Damage Detection for Wooden Components of Ancient Chinese Building*, Ph.D. Dissertation, Beijing University of Technology, Beijing, China.
- Morales-Conde, M. J., and Machado, J. S. (2017). "Evaluation of cross-sectional variation of timber bending modulus of elasticity by stress waves," *Construction and Building Materials* 134, 617-625. DOI: 10.1016/j.conbuildmat.2016.12.188
- Wang, C. (2019). "Application and research of optimal projection Pursuit Model in hydraulic modernization evaluation," *Heilongjiang Hydraulic Science and Technology* 47(12), 205-208.
- Wang, Z., Ma, D., Qian, W., Wang W., Guo, X., Xu, Q., Huan, J., and Gao, Z. (2019). "Detection and prediction of internal damage in the ancient timber structure based on optimal combined model," *Advances in Civil Engineering* 2019, 1-18. DOI: 10.1155/2019/7108262
- Wang, Z., Wang, W., Ma, D., Guo, X., Huan, J., and Cheng, L. (2020). "Coupling model of fuzzy soft set and Bayesian method to forecast internal defects of ancient wooden structures based on nondestructive test," *BioResources* 15(1), 1134-1153. DOI: 10.15376/biores.15.1.1134-1153
- Xu, H., Wang, L., You, X., Liu, Y., and Yang, X. (2011). "Propagation velocity of stress wave and ultrasonic wave transmitting on indefectible cross section of standing trees," *Scientia Silvae Sinicae* 47(4), 129-134.
- Yue, X., Wang, L., Wacker, A. P., and Zhu, Z. (2019). "Electric resistance tomography

- and stress wave tomography for decay detection in trees-a comparison study,” *PeerJ* 7, 1-16. DOI: 10.7717/peerj.6444
- Zhang, Q., Wang, J., and Li, B. (2015). “Prediction method of loess collapsibility based on fuzzy analogy preferred ratio,” *Yangtze River* 46(1), 90-93.
- Zhao, W. and He, Y.-L. (2008). “Case-based reasoning approach to stability evaluation of structured rock slope,” *Journal of Railway Engineering Society* 25(7), 5-9.
- Zhou, L., Wang, W., and Ma, R. (2010) “Application of method of entropy proportion to urban earthquake disaster risk index,” *Earthquake Engineering and Engineering Vibration* 30(1), 93-97.

Article submitted: March 23, 2021; Peer review completed: May 1, 2021; Revised version received and accepted: May 10, 2021; Published: May 11, 2021.
DOI: 10.15376/biores.16.3.4814-4830